Entropy Generation and Natural Convection in a Square Cavity with a Horizontal Partition and a Heated Square Block

Ahmed El Hamri[1(✉)], Mustapha Mahdoui[1], Fatima Bahraoui[1], Xavier Chesneau[2], and Belkacem Zeghmati[2]

[1] Thermal and Energy Transfer Laboratory, Physics Department, Faculty of Science and Technology of Tangier, Tangier, Morocco
ahmed.elhamri1@etu.uae.ac.ma

[2] LAMPS EA4217, University of Perpignan Via Domitia, Perpignan, France

Abstract. The present work is dedicated to a numerical investigation of natural convection in a differentially heated square enclosure with a solid partition attached to the heated wall and a heating block freely positioned in the cavity. In this study, the length of the solid wall, the position of the heating block, and the Rayleigh numbers of 10^3, 10^4, and 10^5 are investigated for seven different positions of the heating block and three different lengths of the solid partition. The finite difference method through the concept of vorticity-stream function formulation has been applied. The results clearly show that when the heated block is moved towards the cold wall, the average value of the Nusselt number decreases. For high Rayleigh numbers, the average value of the Nusselt number varies proportionally and inversely with the length of the solid partition when the heated block is positioned after or before position 4 respectively. The positive influence of the heated block on the average Nusselt number can be seen when the heated block is moved to the upper heated part of the cavity. The entropy generation is maximum at position 4 for all scenarios.

Keywords: Natural convection · Heated block · Solid partition · Entropy generation · Nusselt number · Rayleigh number

1 Introduction

Natural convection has gained significant attention in recent years due to its impact on various applications like electronics cooling, thermal management of battery modules, solar heating and cooling, power generation, and solar dryer. Researchers have conducted studies on natural convection using different geometries and boundary conditions, both theoretically and experimentally. One example is the study by Merrikh et al. [1] who looked at the natural convection inside a square enclosure filled with solid blocks and a saturated fluid. They found that the heat transfer is slowed if the number of solid blocks is less than the minimum required for flow transmission. Similarly, Tilehnoee et al. [2] studied the free convective flow, heat transmission, and entropy formation of

F. Ali-Toudert et al. (Eds.): JITH 2022, LNME, pp. 249–259, 2024.
https://doi.org/10.1007/978-3-031-43934-6_26

liquid sodium in a heated square enclosure with cylindrical solid blocks. They found that increasing the Rayleigh number leads to an increase in the average Nusselt number and entropy production. Garoosi et al. [3] conducted a numerical study on the heat transfer performance of nano-fluids in square enclosures. They found that the heat transfer rate decreases at low Rayleigh numbers but increasing the number of nanoparticles, the vertical orientation of the conductive partition, and the size of the solid barrier can improve the heat transfer rate. Kalidasan et al. [4] studied the natural laminar convection inside an open C-shaped cavity using the vorticity-stream function approach. They found that as the Rayleigh number increases, the intensity of the primary vortex decreases and heat transfer improves with an increase in the fraction of hybrid nano-composites. Bhave et al. [5] conducted a parametric study of natural convection in a square enclosure with differentially heated vertical walls, adiabatic horizontal walls, and an adiabatic solid block. They found that increasing the size of the block reduces the thermal mass of the fluid and decreases wall heat transfer. Gangawane et al. [6] studied the mixed convection in a lid-driven semicircular cavity and found that a triangle block performs better in terms of heat transmission. Mouhtadi et al. [7] looked at the natural convection of air in a horizontal channel with evenly spaced heating blocks. They found that the Rayleigh number and the type of solution have a significant impact on the heat transfer. Farkach et al. [8] proposed a computational approach for modeling natural convection in annulus space with a partially heated inner cylinder. They found that the Nusselt number increases with an increase in the Rayleigh number and radius ratio. Siavashi et al. [9] studied the natural convection of a Cu-water nanofluid in a cavity with porous fins on its hot wall. They found that the number of fins reduces entropy production and a low concentration of nanoparticles improves heat transfer. Rahimi et al. [10] studied the impact of a rigid body inside a cavity filled with nanofluid water and found that the total entropy generation has a direct and inverse connection with the Rayleigh number and solid volume percentage. Al-Kouz et al. [11] studied entropy production in the steady-state laminar two-dimensional flow of air-Al_2O_3 nanofluid in a square cavity with two solid fins at the hot wall. They found that entropy production decreases as the Rayleigh number approaches 10^4. Abbassi and Zeghmati [12] studied the natural magneto hydrodynamic convection of nano-fluids in an incinerator-shaped enclosure. They found that increasing the height and width of the heating element, the volume fraction of nanoparticles, and the Rayleigh number increases entropy generation.

With this quick bibliographic review, we can conclude that there is a lack of information on the cooling of electronic systems with a multiple heated partition. Moreover, these elements, as main units in electronic devices, should be considered comprehensively. Therefore, the analysis of this study is conducted in a square enclosure. We investigate the influence of Rayleigh number and the position of the square block with a horizontal partition. On the other hand, this study also focuses on entropy generation as an optimization parameter for a realistic development of such a passive cooling system. Such a cooling system and the performance of the attached electronic components can be affected by the high value of irreversibility of heat transfer or fluid friction.

2 Physical Model and Mathematical Formulation

2.1 Physical Model

Figure 1 shows the physical model that consists of differentially heated square cavity of dimension L with a partition of length w and width e attached to the heated wall. The horizontal walls are adiabatic while the vertical walls are held at hot (T_h) and cold (T_c) temperatures. The cavity also contains a square block of dimension 0.1 × L at a uniform temperature. In addition, Fig. 1b illustrates the different cases that will be examined in this study. We assumed the transfers in the cavity laminar and two-dimensional, the thermal properties of the air are constants excepted the density variation in the buoyancy term which obeys to the Boussinesq approximation.

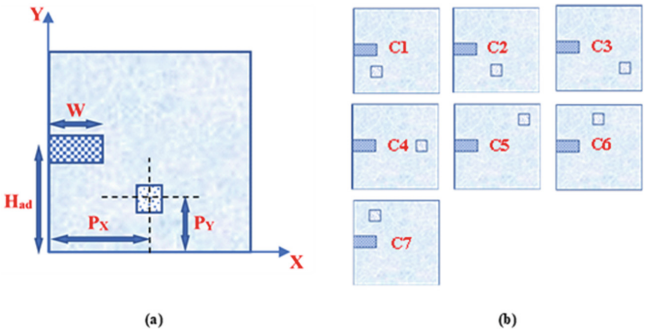

Fig. 1. **a** Physical model; **b** cases taken into consideration

2.2 Mathematical Formulation

The dimensionless equations of the conservation of mass, momentum and energy (in the fluid and in the solid) in Cartesian coordinates can be written using the vorticity-stream function formulation as illustrated in literature [13] as follow:

$$\Omega = -\nabla^2 \Psi \tag{1}$$

$$\frac{\partial \Omega}{\partial \tau} + U\frac{\partial \Omega}{\partial X} + V\frac{\partial \Omega}{\partial Y} = \Pr .\nabla^2 \Omega + Ra \cdot Pr \cdot \frac{\partial \theta}{\partial Y} \tag{2}$$

$$\frac{\partial \theta}{\partial \tau} + U\frac{\partial \theta}{\partial X} + V\frac{\partial \theta}{\partial Y} = \nabla^2 \theta \tag{3}$$

$$\frac{\partial \theta}{\partial \tau} = \frac{\alpha_S}{\alpha}\nabla^2 \theta \tag{4}$$

The dimensionless parameters in the Eqs. (1)–(4) are defined as follow:

$$X = \frac{x}{L}, \quad Y = \frac{y}{L}, \quad W = \frac{w}{L}, \quad B = \frac{b}{L}, \tau = \frac{t\alpha}{L^2}, H_{ad} = \frac{H}{L} \tag{5}$$

$$U = \frac{uL}{\alpha}, \quad V = \frac{vL}{\alpha}, \quad \theta = \frac{T - T_h}{T_c - T_h}, \quad \Psi = \frac{\psi}{\alpha}, \quad \Omega = \frac{\omega L^2}{\alpha} \tag{6}$$

$$\mathrm{Pr} = \frac{\nu}{\alpha}, \quad Ra = \frac{g\beta L^3 (T_h - T_c)}{\nu\alpha} \tag{7}$$

$\mathrm{Pr} = \nu/\alpha$ is the Prandtl number, and Ra is the Rayleigh number. B and W are the dimensionless length and thickness of solid partition, respectively. The generation of entropy as defined in literature by Hakan et al. [14] and the Nusselt number are defined as follows.

$$\begin{aligned} N_S &= \left[\left(\frac{\partial\theta}{\partial \mathrm{X}}\right)^2 + \left(\frac{\partial\theta}{\partial \mathrm{Y}}\right)^2\right] + \gamma \left\{ \begin{array}{l} \left[\left(\frac{\partial \mathrm{U}}{\partial \mathrm{X}}\right)^2 + \left(\frac{\partial \mathrm{V}}{\partial \mathrm{Y}}\right)^2\right] \\ +\left(\frac{\partial \mathrm{V}}{\partial X} + \frac{\partial \mathrm{U}}{\partial \mathrm{Y}}\right)^2 \end{array} \right\}, Nu_{local} \\ &= -\frac{\partial\theta}{\partial n}\bigg|_{\text{surface}} dn \end{aligned} \tag{8}$$

With $\gamma = \frac{\mu\alpha^2(T_c+T_h)}{2\kappa\Delta T^2 L^2}$ is irreversibility distribution ratio. The local entropy is obtained from the dimensionless form using the following formula:

$$N_s = S_{gen}\frac{1}{k}\left(\frac{lT_c}{\Delta T}\right)^2 \tag{9}$$

The first terms in the dimensionless local entropy generation represent the dimensionless heat transfer irreversibility, and the last terms indicates the dimensionless irreversibility due to the fluid friction. The average Nusselt number was calculated by integrating the local Nusselt number over all the heated walls of the cavity and solid partition, we define the average Nusselt number on the heat part of the cavity as follow:

$$Nu_{av} = \int_0^{2w+1} -\frac{\partial\theta}{\partial n}\bigg|_{\text{surface}} dn \tag{10}$$

We associated to Eqs. (1)–(4) the dimensionless initials and boundary conditions.

- Initial condition:
  - For $\boldsymbol{\tau} \leq \boldsymbol{\tau}_0$, for all X and Y in domain:

$$U = 0, V = 0, \Psi = 0, \theta = 0 \tag{11}$$

- Boundary conditions:
  - For $\boldsymbol{\tau} > \boldsymbol{\tau}_0$

    $\boldsymbol{X} = 0, 0 < \boldsymbol{Y} < 1$

$$U = V = 0, \Psi = 0, \theta = 1, \Omega = -\frac{\partial^2\Psi}{\partial X^2} \tag{12}$$

$\boldsymbol{X} = 1, 0 < \boldsymbol{Y} < 1$

$$U = V = 0, \Psi = 0, \theta = 0, \Omega = -\frac{\partial^2 \Psi}{\partial X^2} \tag{13}$$

$\boldsymbol{Y} = 0, 0 < \boldsymbol{X} < 1$

$$U = V = 0, \Psi = 0, \frac{\partial \theta}{\partial Y} = 0, \Omega = -\frac{\partial^2 \Psi}{\partial Y^2} \tag{14}$$

$\boldsymbol{Y} = 1, 0 < \boldsymbol{X} < 1$

$$U = V = 0, \Psi = 0, \frac{\partial \theta}{\partial Y} = 0, \Omega = -\frac{\partial^2 \Psi}{\partial Y^2} \tag{15}$$

$\boldsymbol{X} = \boldsymbol{P_X} - \frac{\boldsymbol{B}}{2}$ *and* $\boldsymbol{X} = \boldsymbol{P_X} + \frac{\boldsymbol{B}}{2}$,

$$U = V = 0, \Psi = 0, \theta = 1, \Omega = -\frac{\partial^2 \Psi}{\partial X^2} \tag{16}$$

$\boldsymbol{Y} = \boldsymbol{P_Y} - \frac{\boldsymbol{B}}{2}$ *and* $\boldsymbol{Y} = \boldsymbol{P_Y} + \frac{\boldsymbol{B}}{2}, \boldsymbol{P_X} - \frac{\boldsymbol{B}}{2} \le \boldsymbol{X} \le \boldsymbol{P_X} + \frac{\boldsymbol{B}}{2}$

$$U = V = 0, \Psi = 0, \theta = 1, \Omega = -\frac{\partial^2 \Psi}{\partial Y^2} \tag{17}$$

$\boldsymbol{X} = 0, \boldsymbol{H_{ad}} - \frac{\boldsymbol{B}}{2} \le \boldsymbol{Y} \le \boldsymbol{H_{ad}} + \frac{\boldsymbol{B}}{2}$

$$\theta = 1 \tag{18}$$

$\boldsymbol{X} = \boldsymbol{W}, \boldsymbol{H_{ad}} - \frac{\boldsymbol{B}}{2} \le \boldsymbol{Y} \le \boldsymbol{H_{ad}} + \frac{\boldsymbol{B}}{2}$

$$U = V = 0, \Psi = 0, \left(\frac{\partial \theta}{\partial X}\right)_f = \frac{\kappa_s}{\kappa_f}\left(\frac{\partial \theta}{\partial X}\right)_s, \Omega = -\frac{\partial^2 \Psi}{\partial X^2} \tag{19}$$

$0 \le \boldsymbol{X} \le \boldsymbol{W}, \boldsymbol{Y} = \boldsymbol{H_{ad}} - \frac{\boldsymbol{B}}{2}, \quad \boldsymbol{Y} = \boldsymbol{H_{ad}} + \frac{\boldsymbol{B}}{2}$

$$U = V = 0, \Psi = 0, \left(\frac{\partial \theta}{\partial Y}\right)_f = \frac{\kappa_s}{\kappa_f}\left(\frac{\partial \theta}{\partial Y}\right)_s, \Omega = -\frac{\partial^2 \Psi}{\partial Y^2} \tag{20}$$

2.3 Numerical Procedure

The finite difference method was used to discretize Eqs. (1–4). The convection terms were calculated with a centered difference scheme and the time derivatives were calculated with a fully implicit scheme. The grid was uniform and the nonlinear algebraic equations were solved using the successive over-relaxation method for Eq. (1) and Thomas algorithm for Eqs. (2–4). The mesh size was 200×200 and the time step was 10^{-4}. The steady state solution was found by using a convergence criterion for each time step.

$$\left|\frac{Nu_{av}^{t+\Delta\tau} - Nu_{av}^{t}}{Nu_{av}^{t}}\right| < 10^{-8} \tag{21}$$

The numerical code was tested on a simple, differentially heated cavity, which has been studied in previous literature [15–17]. The results were visually validated using streamlines and isotherms (Fig. 2, Nag et al. [18]). The maximum vertical velocity (V_m) and average Nusselt number were evaluated under steady state. The code was run with 4 different Rayleigh numbers (10^3, 10^4, 10^5, 10^6) and the results agreed with previous studies, with a maximum discrepancy of 3% for V_m and 2.23% for the average Nusselt number (Table 1 and Fig. 2).

Table 1. Maximum velocity and average Nusselt values.

Vmax	$Ra = 10^3$	$Ra = 10^4$	$Ra = 10^5$	$Ra = 10^6$	Maximal ERR %
de Vahl Davis [15]	3.697	19.62	68.59	219.36	0.85
Ramaswamy et al. [16]		19.62	68.60	221.54	0.25
Present study	3.701	19.637	68.428	221.232	
Nuav					
de Vahl Davis [15]	1.117	2.238	4.509	8.817	2.23
Present study	1.121	2.247	4.529	8.882	
Markatos and Pericleous [17]	1.108	2.201	4.43	8.754	

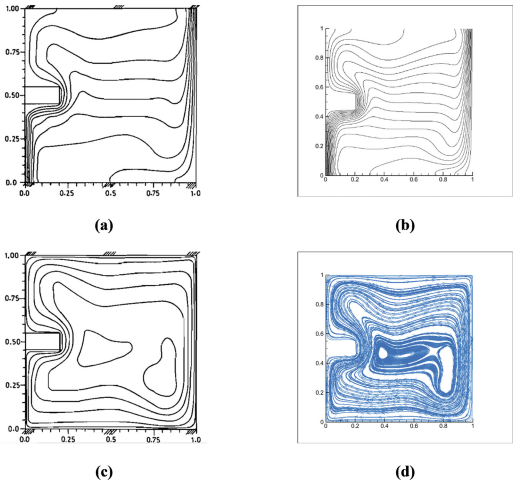

Fig. 2. Comparison of streamlines and isotherms of the present work (**b**, **d**) and Nag et al. [18] (**a**, **c**)

3 Results and Discussion

The flow structure in a cavity is determined by multiple factors. The balance between buoyancy and viscous forces has a significant impact on the aeraulic flow, the presence and strength of vortices, and their position. This is demonstrated by Fig. 3, where a third vortex is seen at the bottom of the heating block with a higher Rayleigh number. The weak vortices in configuration 6 at Ra = 10^3 are replaced by a stronger vortex at Ra = 10^5. The Rayleigh number determines the air flow in areas dominated by viscous forces. The maximum current function value decreases with an increase in the length of the horizontal partition. This intensifies the viscous force and confines the air near the partition. The vortex between the solid partition and heating block is due to the temperature gradient between them. Modifying the partition length moves the main vortex towards the partition and limits the fluid to the lower part of the cavity, reducing heat transfer in the area.

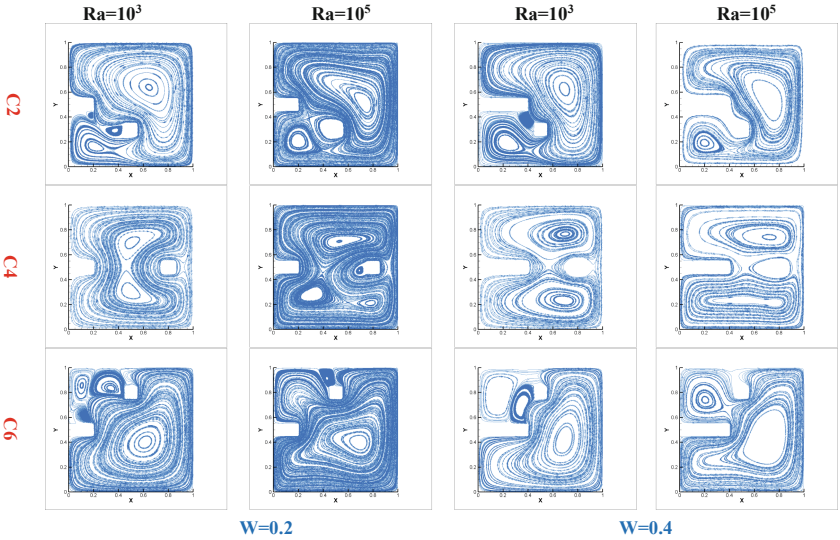

Fig. 3. Streamlines distribution for 3 typical configurations (2, 4 and 6) at Rayleigh number Ra = 10^3, 10^5 and solid partitions dimensionless length W = 0.2 and 0.4.

The effect of the Rayleigh number, heating block position, and solid partition length are analyzed. As shown in Fig. 4, high Rayleigh numbers result in a larger temperature gradient near the solid partition and increased heat transfer. However, increasing the partition length negatively impacts the isotherm density in these regions. The heating block near the cold wall increases isotherm density along the wall and improves heat transfer. The heating block near the hot wall also improves heat transfer, while being on the vertical wall reduces it. Moving the heating block to the upper area of the solid partition increases isotherm density in the lower area, leading to improved heat transfer in the lower part of the cavity.

This section discusses the results on entropy generation and average Nusselt number. The entropy generation is mainly caused by temperature and velocity gradients within the cavity. It includes both heat transfer irreversibility and fluid friction irreversibility. In natural convection, the entropy generation is mainly due to temperature gradients as air velocities are low. The maximum local entropy generation was found at the right face of the heating block (Fig. 5). It increases as one approaches the cold wall. The fluid friction irreversibility is reduced when the heating block is near the middle of the cold wall, due to the low velocity gradient. It is highest when the heating block is close to the solid partition.

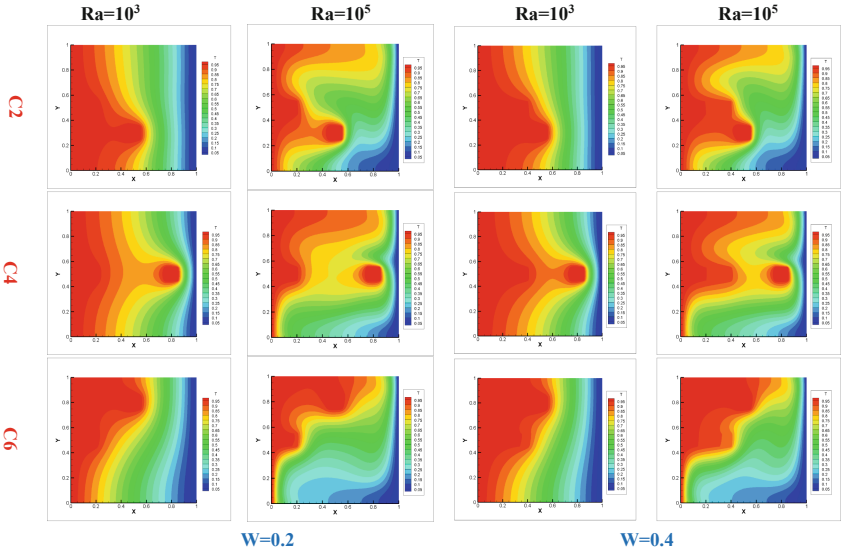

Fig. 4. Isotherms for 3 typical configurations (2, 4 and 6) at Rayleigh number Ra $= 10^3, 10^5$ and solid partitions dimensionless length W $= 0.2$ and 0.4.

The Nusselt number along the heated wall is calculated using local Nusselt number, partition length, Rayleigh number, and heating block position. The results are shown in Fig. 6. For low Rayleigh number and W $= 0.1$, position 2 has the lowest average Nusselt number due to preheated air. Increasing the partition length improves heat transfer but position 4 still has low heat transfer. Position 3 is the worst for high Rayleigh numbers due to preheating. The best position in the study is position 7.

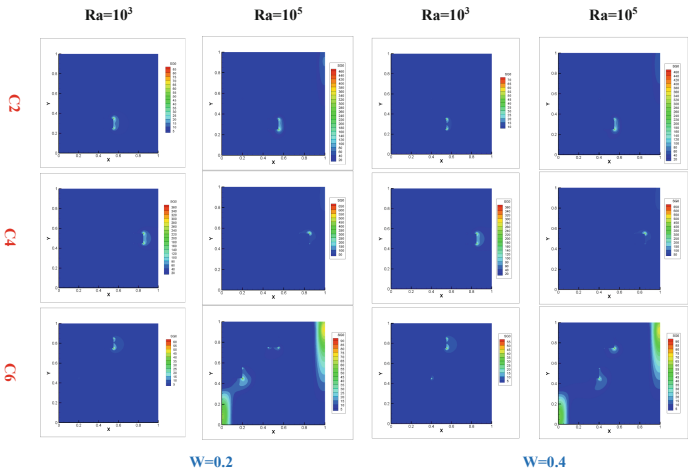

Fig. 5. Entropy generation distribution

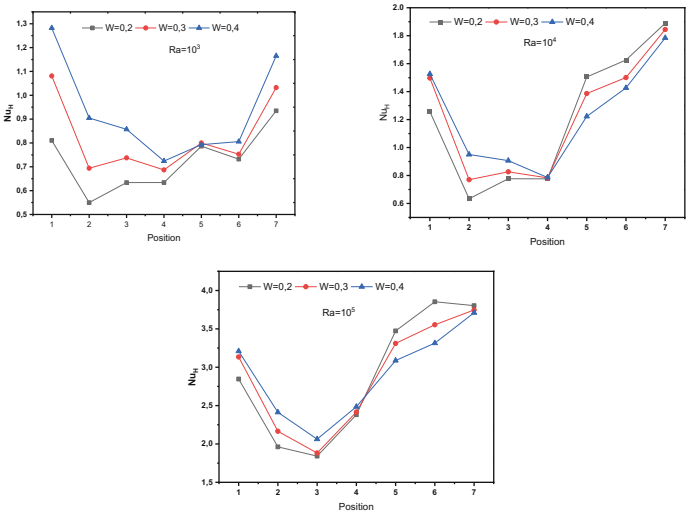

Fig. 6. Average Nusselt number evolution versus the position of the heating block. Effects of Ra and of the partition length

4 Conclusion

Natural convection in a differentially heated square cavity with a locally heated block of uniform temperature freely positioned in the cavity under the influence of a solid partition attached to the heated wall was studied numerically. The governing equations were discretized using the finite difference method with dimensionless stream function and vorticity variables. The effects of the Rayleigh number, solid partition length, and heated block position on streamline, isotherms, entropy production, and the average

Nusselt number have been investigated. Following the results of this work, we can conclude that moving the heated block beyond the solid partition and increasing the length of the solid partition leads to an overall improvement of the convective flow in the heated part.

References

1. Merrikh, A.A., Lage, J.L.: Natural convection in an enclosure with disconnected and conducting solid blocks. Int. J. Heat Mass Transf. **48**, 1361–1372 (2005)
2. Hashemi-Tilehnoee, M., del Barrio, E.P., Seyyedi, S.M.: Magneto-turbulent natural convection and entropy generation analyses in liquid sodium-filled cavity partially heated and cooled from sidewalls with circular blocks. Int. Commun. Heat Mass Transf. **134**, 106053 (2022)
3. Garoosi, F., Talebi, F.: Numerical simulation of conjugate conduction and natural convection heat transfer of nanofluid inside a square enclosure containing a conductive partition and several disconnected conducting solid blocks using the Buongiorno's two phase model. Powder Technol. **317**, 48–71 (2017)
4. Kalidasan, K., Velkennedy, R., Rajesh Kanna, P.: Laminar natural convection of Copper—Titania/Water hybrid nanofluid in an open ended C—shaped enclosure with an isothermal block. J. Mol. Liq. **246**, 251–258 (2017)
5. Bhave, P., Narasimhan, A., Rees, D.A.S.: Natural convection heat transfer enhancement using adiabatic block: optimal block size and Prandtl number effect. Int. J. Heat Mass Transf. **49**, 3807–3818 (2006)
6. Gangawane, K.M., Oztop, H.F.: Mixed convection in the heated semi-circular lid-driven cavity for non-Newtonian power-law fluids: effect of presence and shape of the block, Chinese. J. Chem. Eng. **28**, 1225–1240 (2020)
7. Mouhtadi, D., Amahmid, A., Hasnaoui, M., Bennacer, R.: Natural convection in a horizontal channel provided with heat generating blocks: discussion of the isothermal blocks validity. Energy Convers. Manag. **53**, 45–54 (2012)
8. Farkach, Y., Derfoufi, S., Ahachad, M., Bahraoui, F., Mahdaoui, M.: Numerical investigation of natural convection in concentric cylinder partially heated based on MRT-lattice Boltzmann method. Int. Commun. Heat Mass Transf. **132**, 105856 (2022)
9. Siavashi, M., Yousofvand, R., Rezanejad, S.: Nanofluid and porous fins effect on natural convection and entropy generation of flow inside a cavity. Adv. Powder Technol. **29**, 142–156 (2018)
10. Rahimi, A., Kasaeipoor, A., Malekshah, E.H.: Lattice Boltzmann simulation of natural convection and entropy generation in cavities filled with nanofluid in existence of internal rigid bodies-experimental thermo-physical properties. J. Mol. Liq. **242**, 580–593 (2017)
11. Al-Kouz, W., Al-Muhtady, A., Owhaib, W., Al-Dahidi, S., Hader, M., Abu-Alghanam, R.: Entropy generation optimization for rarified nanofluid flows in a square cavity with two fins at the hot wall. Entropy, 21 (2019)
12. Abbassi, M.A., Safaei, M.R., Djebali, R., Guedri, K., Zeghmati, B., Alrashed, A.A.A.A.: LBM simulation of free convection in a nanofluid filled incinerator containing a hot block. Int. J. Mech. Sci. **148**, 393–408 (2018). https://doi.org/10.1016/j.ijmecsci.2018.04.057
13. Mobedi, M.: Conjugate natural convection in a square cavity with finite thickness horizontal walls. Int. Commun. Heat Mass Transf. **35**, 503–513 (2008)
14. Oztop, H.F., Al-Salem, K.: A review on entropy generation in natural and mixed convection heat transfer for energy systems. Renew. Sustain. Energy Rev. **16**, 911–920 (2012)
15. De Vahl Davis, G.: Natural convection of air in a square cavity: a bench mark numerical solution. Int. J. Numer. Methods Fluids. **3**, 249–264 (1983)

16. Ramaswamy, B., Jue, T.C., Akin, J.E.: Semi-implicit and explicit finite element schemes for coupled fluid/thermal problems. Int. J. Numer. Methods Eng. **34**, 675–696 (1992)
17. Markatos, N.C., Pericleous, K.A.: Laminar and turbulent natural convection in an enclosed cavity. Int. J. Heat Mass Transf. **27**, 755–772 (1984)
18. Nag, A., Sarkar, A., Sastri, V.M.K.: Effect of thick horizontal partial partition attached to one of the active walls of a differentially heated square cavity. Numer. Heat Transf. Part A Appl. **25**, 611–625 (1994)